

# Engineering Notes

*ENGINEERING NOTES are short manuscripts describing new developments or important results of a preliminary nature. These Notes cannot exceed six manuscript pages and three figures; a page of text may be substituted for a figure and vice versa. After informal review by the editors, they may be published within a few months of the date of receipt. Style requirements are the same as for regular contributions (see inside back cover).*

## Mars Entry Simulation Using an Inductively Heated Plasma Generator

G. Herdrich,\* M. Auweter-Kurtz,<sup>†</sup>

P. Endlich,<sup>‡</sup> and H. Kurtz<sup>§</sup>

University of Stuttgart, D-70550 Stuttgart, Germany

### Introduction

**E**LECTRODELESS inductively heated plasma generators enable basic thermal protection system material tests (e.g., catalyticity) and the simulation of atmospheres such as of Mars or Venus. The generators have an optimized design, where the induction coil is closer to the plasma than it is with other designs. Therefore, the electromagnetic field loss is reduced. The water-cooling system surrounds both the coil and the plasma tube. The design of inductively heated plasma generator (IPG) 4, the associated plasma wind tunnel, and experimental results using CO<sub>2</sub> are described. Test cases characterizing the power balances are demonstrated, leading to rough estimations of the plasma temperature. Additionally, heat-flux profiles are shown for the newly developed prototype plasma generator equipped with a graphite nozzle. The values are taken at lower power modes reaching typical Mars scenario values of 0.5 MW/m<sup>2</sup> and more. The total pressures are in the order of 1 kPa, that is, typical values as expected for the well-known Mars Sample Return Mission or the balloon mission of Mars Society. A powder feeder is available to simulate the dust particles in the Martian atmosphere. Here, preliminary tests with O<sub>2</sub>-plasmas were performed using metal particles to get an understanding of the operational behavior of the facility.

Concurrently, there are a lot of planetary probe missions, soft landing missions, and sample return missions such as Venus Sample Return Mission, Mars Mini-Probes,<sup>1,2</sup> Mars Society Balloon Mission,<sup>3</sup> or Mars Sample Return Mission.<sup>4</sup> For such missions both thermal protection system (TPS) and environment (plasma) during the entry have to be investigated by means of computational and ground-facility-based simulations. Such ground facilities are the IRS plasma wind tunnels PWK 1-5, reproducing the thermal, aerodynamic, and chemical load on the surface of a space vehicle entering an atmosphere. They are operated with different plasma generators.<sup>5-9</sup>

Received 29 August 2001; revision received 3 July 2002; accepted for publication 28 April 2003. Copyright © 2003 by the authors. Published by the American Institute of Aeronautics and Astronautics, Inc., with permission. Copies of this paper may be made for personal or internal use, on condition that the copier pay the \$10.00 per-copy fee to the Copyright Clearance Center, Inc., 222 Rosewood Drive, Danvers, MA 01923; include the code 0022-4650/03 \$10.00 in correspondence with the CCC.

\*Research Engineer and Ph.D. Student, Institute of Space Systems, Pfaffenwaldring 31; herdrich@irs.uni-stuttgart.de. Member AIAA.

<sup>†</sup>Professor and Leader Space Transportation Division, Institute of Space Systems, Pfaffenwaldring 31. Associate Fellow AIAA.

<sup>‡</sup>Research Engineer and Ph.D. Student, Institute of Space Systems, Pfaffenwaldring 31.

<sup>§</sup>Head of IRS Laboratory, Institute of Space Systems, Pfaffenwaldring 31.

Inductively heated facilities for entry simulation exist in France, Belgium, and Russia.<sup>10-12</sup> Test with CO<sub>2</sub> are documented by the Institute for Problems in Mechanics of the Russian Academy of Science in Moscow.<sup>11</sup> The facility in France is used with argon and air as working gases. With the Belgian facility CO<sub>2</sub> tests were performed as well. This facility has a so-called cold-cage technology, where erosion in the plasma generator is expected. In comparison with a lot of the inductively heated generators such as described in Ref. 10, the cold cage, a water-cooled copper frame lying within the plasma container (e.g., a quartz tube), is absent. The Institute of Space Systems-IPGs (IRS-IPGs) have no cold cage. This ensures that no metallic erosion from parts exposed to the plasma can appear.

Nonintrusive measurement techniques like emission spectroscopy, Fabry–Perot interferometry, and laser-induced fluorescence are used to investigate the plasma flows.<sup>13</sup> They are applied to determine atomic and molecular density and the velocity distribution in the boundary layer. The laser absorption spectroscopy technique of the Department of Aeronautics and Astronautics, Tokyo University, was used for IRS-PWK3 to determine number densities and translational temperatures, for example, of O<sub>2</sub>.<sup>14</sup>

Besides the nonintrusive measurement techniques, mass spectrometry, electrostatic and radiation probes belong to the group of intrusive measurement techniques. Mechanical probes are among the most important instruments for plasma-diagnostic measurements and are often used. Besides the standard sample support system, which carries the TPS material sample to be tested, probes for pitot pressure, Mach number, heat flux, enthalpy, and oxygen partial pressure determination are used. Electrostatic probes are used to ascertain the plasma potential, electron density and temperature, energy distribution of the electrons, ion temperature, and flow velocity. Radiometric probes are unavoidable when the radiation heat flux cannot be neglected compared to the convective part. This is the case when during sample return missions the entry speed into the Earth's atmosphere is especially high or when the atmosphere of another celestial body (which is to be entered) contains strong radiating species, as, for example, the atmosphere of Titan. An overview for the IRS plasma diagnostic tools is given in Ref. 13.

### Setup of PWK3 and the IPG

The facility consists of the IPG and the vacuum chamber and has already been described.<sup>15</sup> It is about 2 m in length and 1.6 m in diameter. Optical accesses to the chamber enable the measurement of the plasma. A heat exchanger at the end of the chamber protects the vacuum system from being damaged. The flat lid of PWK3 is equipped with the IPG and the connected capacitors.

The right-side flange of the vacuum chamber is connected to the IRS vacuum pump system, which simulates pressures at altitudes up to 90 km (Earth). Total suction power of the pumps amounts to 6.000 m<sup>3</sup>/h at atmospheric pressure and reaches about 250.000 m<sup>3</sup>/h at 10 Pa measured at the intake pipe of the system, which has a diameter of 1 m. The base pressure is 0.5 Pa. The desired tank pressure can be adjusted between the best achievable vacuum and 100 kPa by removing one or more pumps from the circuit and/or mixing additional air into the system close to the pumps. A powder feeder is available for the simulation of dust particles during Mars entry.

It is known that CO<sub>2</sub> requires a deactivation using a suitable gas such as N<sub>2</sub> as the produced CO can create an explosive mixture that especially could endanger the zones of higher pressure of the facility, that is, parts of the vacuum pump system. Hence, all CO<sub>2</sub>

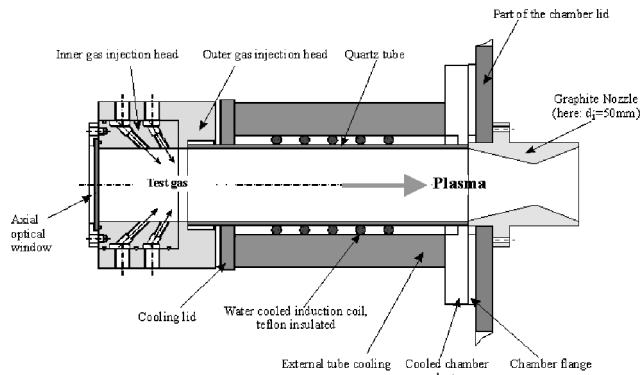


Fig. 1 View of the plasma source IPG4.

experiments are carried out using an injection of  $N_2$  at the right-side flange of the chamber. Common studies<sup>16–18</sup> point out that the ignition regime for CO is between 12.5 and 74 (volumetric relative shares). Furthermore, the deactivating of CO requires a volumetric share of  $O_2$  lower than 5%. If the maximum production of CO (total dissociation of  $CO_2$ ) is assumed, the required deactivating gas  $N_2$  can be calculated, which leads to the need that 5.4 g/s  $N_2$  deactivate a plasma derived from 1 g/s  $CO_2$ .

The external resonant circuit is water cooled. With this, the coil and the capacitors, which have a capacity of  $6 \text{ nF} \pm 20\%$  each, are cooled. The resonant circuit is built in Meissner-type switching using a metal-ceramic triode with an oscillator efficiency of about 75% (Ref. 15). Its nominal frequency can be changed by switching the number of capacitors as well as by the use of coils with different inductivities. The circuit is switched to a 375-kW power supply.

The alternating current in the coil induces a mostly azimuthal electric field inside the tube. This electric field initiates an electric discharge in the gas that is injected at one side into the tube (Fig. 1). The produced plasma is expanded into the vacuum chamber. The plasma current amplitude, and thus the ohmic heating, strongly depends on the electric conductivity of the plasma and the resonant frequency.

An axial optical access through the inner injection head enables investigations of the plasma inside the generator (Fig. 1). The tube-cooling system is transparent; hence, the position of the plasma flame in the tube can be observed with regard to different operating parameters such as chamber pressure, gas, mass flow, and anode power. This cooling system is quite unique in terms of design and its transparency. The design enables a minimization of field losses. The observation of the plasma is supported by the axial optical window. The quartz tube contains the produced plasma, which leaves the generator through the water-cooled chamber adapter and sustains very high operational powers.<sup>7</sup> The induction coil is connected to the external resonant circuit delivering power and cooling water for the IPG.

The length of IPG4 is about 0.46 m. First investigations with  $CO_2$  were done with the IPG4 prototype configuration using graphite nozzles<sup>8</sup> and a water-cooled brass/copper nozzle. The nozzle consists of three modular parts such that the inner nozzle geometry (throat diameter) can be easily changed as the cooling water channel is milled into the outer part of the nozzle. The modular design of IPG4 enables the use of different types of nozzles.

### Measurement Techniques

The techniques used for the measurements are described. Related accuracies of the calorimeter and the probes were analyzed and presented in Ref. 7.

#### Operational Parameter of PWK3-IPG3

The resonant circuit is supplied by the dc anode power  $P_A$  (triode's plate power) measured during the operation of the device.<sup>6–9,14,15</sup> The anode voltage  $U_A$  is controlled, and the anode current  $I_A$  results from the plasma load and the accompanying operating con-

ditions. Tube-cooling power and circuit power are measured using resistance thermometers. They are electrically sealed and installed at an acceptable distance from the plasma source to prevent the rf field from disturbing the measurement. The cooling water flow rates are measured. Thermal plasma power is measured with a cavity calorimeter.<sup>7</sup> Mass flow of the test gas and the pressure of the inner gas injection head are measured. A current monitor can be used to determine operational frequencies and coil currents.<sup>19</sup>

#### Cavity Calorimeter

The working principle is quite easy. The plasma enters the cone-shaped copper cavity through a hole. The hole's diameter is 120 mm, which is roughly 25% bigger than the plasma jet diameter. The distance between calorimeter and IPG outlet is about 100 mm. Smaller distances can result in retroactions toward the IPG that manipulate the discharge behavior.<sup>7</sup> Copper is used because of the very high specific heat conductivity and because of its high catalyticity. The copper walls are heated up through radiation, convection, and recombination. The cavity is equipped with spiral copper tubes that guide the cooling water.

With the cooling exit temperature the cooling inlet temperature and the cooling water flow rate measured the plasma power can be calculated:

$$P_{\text{cal}} = \rho_{\text{water}} \dot{V}_{\text{water}} c_{p,\text{water}} (T_{\text{out}} - T_{\text{in}}) \quad (1)$$

Here  $\rho_{\text{water}}$  is the density of the cooling water,  $\dot{V}_{\text{water}}$  is the cooling water flow rate,  $c_{p,\text{water}}$  is the heat capacity,  $T_{\text{out}}$  is the cooling water outlet temperature and  $T_{\text{in}}$  is the cooling water inlet temperature.

The accuracy of calorimeter and heat-flux measurement is in the order of 10% taking into account the accuracies of the applied measurement techniques such as the resistance thermometers and the water flowmeter. This accuracy can be estimated using a differential for  $\Delta P_{\text{cal}}$  with the differences  $\Delta \dot{m}_{\text{water}}$  and  $\Delta (T_{\text{out}} - T_{\text{in}})$ . The heat-flux measurement is less accurate because of the adjustment of the probe and the sensor area accuracy  $\Delta A$  [Eq. (2)].

The pitot probe is geometrically similar to the steady-state heat flux probe (Fig. 2) that was also used for the investigation. The geometries, that is, the outer diameter of 50 mm and the corresponding coupon material sample diameter of 26.5 mm, became the so-called European standard geometry.

The probe area of the calorimeters of the steady-state heat-flux probe (Fig. 2) is given by the front side of small inserts into the front plate of a water-cooled support providing thermal shielding and insulation for other surfaces of the inserts. The inserts consist of a water-cooled tube for steady-state measurements. When the probe is moved into the plasma jet, the heat flux to the insert probe area of the front side facing the plasma is measured. The area of

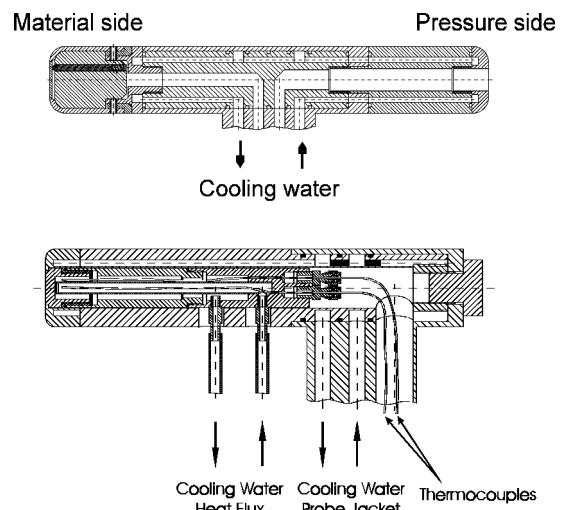


Fig. 2 Pitot-pressure/material probe and steady-state heat-flux probe (European standard).

the insert, which is exposed to the plasma, is similar to the area of a typical material sample:

$$\dot{q} = \frac{c_{p, \text{Water}} \dot{m}_{\text{Water}} (T_{\text{out}} - T_{\text{in}})}{A} \quad (2)$$

### Pyrometer TMR 85H

The temperature of the graphite nozzles was measured using a pyrometer. The measurement wavelength is 900 nm, whereas the spectral emission coefficient of graphite is about 0.85. The temperature measurement range is between 610 and 2600°C. The optical system of the pyrometer is suitable for the geometries that have to be faced by the diameter of the PWK.

## Experimental Results

### IPG4 Operational Behavior (CO<sub>2</sub>)

Experiments within the development of IPG4 were presented in a previous paper.<sup>12</sup> It showed that high-enthalpy CO<sub>2</sub>-plasma flows can be operated steadily. The nozzle throat diameters 40 and 50 mm were found to be feasible in terms of operating the generator without endangering the tube. Three cases were measured using graphite nozzles with 40- and 50-mm throat diameter and the water-cooled nozzle (40-mm throat diameter). All tests were performed with CO<sub>2</sub> plasma using four capacitors and a water-cooled five-turn coil with 0.12 m in length (2 μH,  $f = 0.73$  MHz). The ambient pressure was set to the PWK3 base pressure, which is about 1 hPa under the chosen mass-flow rates. All conditions that were performed for these tests have been made using N<sub>2</sub> to deactivate the hot flow before entering the vacuum system.

To reproduce the thermochemical behavior of a Mars entry, 3% N<sub>2</sub> (volumetric) were injected together with the CO<sub>2</sub> into IPG4. Three different mass-flow rates are distinguished:  $\dot{m}_{\text{CO}_2}$ , that is, the CO<sub>2</sub> mass-flow rate of IPG4 (97%),  $\dot{m}_{\text{N}_2, \text{atm}}$ , that is, the N<sub>2</sub> mass-flow rate of IPG4 (3%),  $\dot{m}_{\text{N}_2, \text{safety}}$ , that is, the deactivating mass flow injected at the end of the chamber.

Three different test cases were investigated:

1) Case 1: A graphite nozzle with 40-mm throat diameter was used. The CO<sub>2</sub> mass-flow rate was 2.2 g/s, the atmospheric N<sub>2</sub> mass flow rate was 44 mg/s, the N<sub>2</sub> safety mass-flow rate was 11.9 g/s, the anode voltage was 6.9 kV, and the discharge power was about 96 kW.

2) Case 2: A graphite nozzle with 50-mm throat diameter was used. The CO<sub>2</sub> mass-flow rate was 2.76 g/s, the atmospheric N<sub>2</sub> mass-flow rate was 52 mg/s, the N<sub>2</sub> safety mass-flow rate was 14.3 g/s, the plate voltage was 7 kV, and the discharge power was about 100 kW.

3) Case 3: The water-cooled nozzle with 40-mm throat diameter was used. The CO<sub>2</sub> mass-flow rate was 2.16 g/s, the atmospheric N<sub>2</sub> mass-flow rate was 43 mg/s, the N<sub>2</sub> safety mass-flow rate was 11.9 g/s, the discharge voltage was 7.1 kV, and the discharge power was about 100 kW.

### Results for Case 1

Figure 3 shows the power balance for IPG4 in operation under the case 1 conditions. A sudden increase of the plasma beam

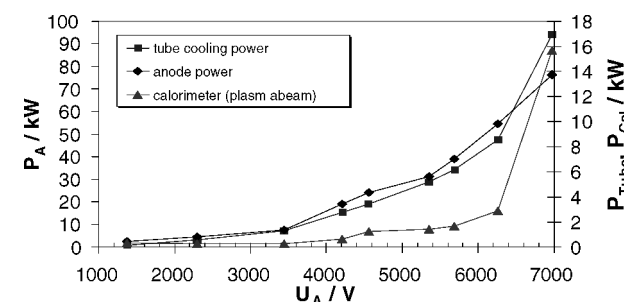


Fig. 3 Anode power, tube-cooling power, and calorimeter power vs anode voltage: case 1.

power can be seen before the final power of 96 kW is reached (between  $U_A = 6.2$  and 7 kV). Simultaneously the plasma becomes very bright. The sudden increase of the thermal powers seem to be caused by the adaption of the plasma as a load for the resonant circuit. This is confirmed by other investigations using oxygen as working gas.<sup>11</sup>

The overall conclusion is that the plasma power is sufficient for Mars entry tests although the thermal losses in terms of tube-cooling power and radiative-cooling-power of the graphite nozzle are quite high. The mean plasma enthalpy is 7 MJ/kg at maximum power, and the mass-flow rate 2.2 g/s. This is, compared with other well-known conditions for O<sub>2</sub> and N<sub>2</sub> plasmas,<sup>11,14</sup> a rather high value. The Future European Space Transportation Program (FESTIP; ESA program for which IRS performed O<sub>2</sub> silicon carbide tests using PWK3-IPG3) condition, for example, has a mean enthalpy of about 5.5 MJ/kg. Considering an efficiency in terms of plasma jet power related to  $P_A$ , we get  $\eta = 0.16$ . Taking into account the anode power of about 100 kW in connection with the tube-cooling power and the nozzle temperature, we have to consider that there are thermal losses higher than 14 kW at the final case 1 condition. However, the achieved mean enthalpy of 7 MJ/kg is sufficient. During the measurement, the nozzle temperature reached almost 1000°C.

### Results for Case 2

Figure 4 depicts the power balance for the IPG4 in operation under case 2 conditions. A sudden increase of the plasma beam power can be seen before the final power of 100 kW is reached (between  $U_A = 7$  and 7.1 kV). This increase can be explained as before as the plasma suddenly becomes a real load to the resonant circuit (see also Ref. 7).

It can be concluded that the measured plasma beam power of about 12.4 kW is sufficiently high for CO<sub>2</sub> TPS material tests. However, the efficiency is 12.3% and, hence, lower than the efficiency of the case 1 condition using the 40-mm nozzle. But the tube-cooling power balance behaves less severe than in case 1 as it does not exceed 13 kW even where the power jump between 7 and 7.1 kV appears.

During the measurement, the nozzle temperature did not exceed 960°C.

### Results for Case 3

The test duration at the maximum anode power of about 100 kW is roughly 300 s. Figure 5 shows the power balance of IPG4. The

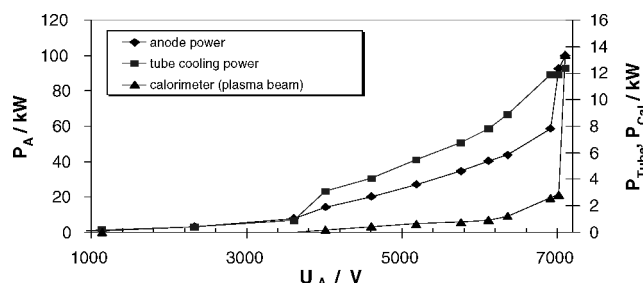


Fig. 4 Anode power, tube-cooling power, and calorimeter power vs anode voltage: case 2.

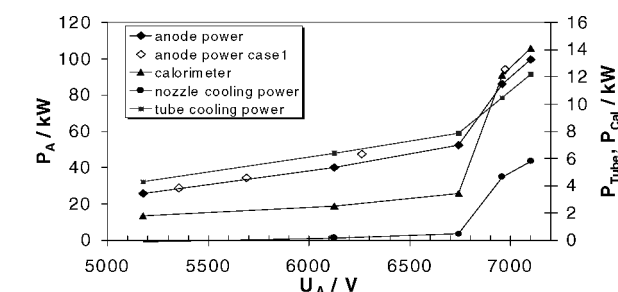


Fig. 5 Anode power, tube-cooling power, nozzle-cooling power, and calorimeter power vs anode voltage: case 3.

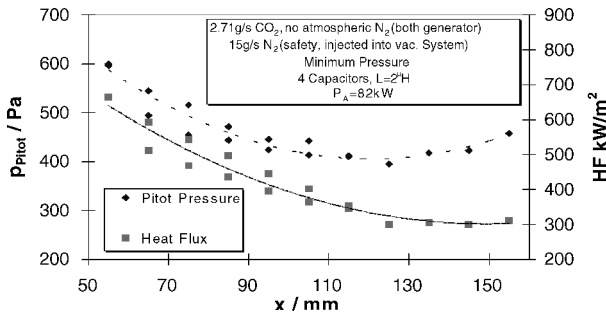


Fig. 6 Heat flux and pitot pressure vs probe distance to generator exit: case 2b.

open symbols show the anode power values of case 1 representing the graphite nozzle with 40-mm inner diameter. It seems that the coupling in both cases is similar.

The anode power related efficiency at maximum  $P_A$  in this case is greater than 14% leading to a mean enthalpy of 6.4 MJ/kg, which is sufficient for the later atmospheric entry test campaigns.

For all conditions typical inner tube pressures are roughly 2 kPa at the high powers. The ratio  $p_{\text{tube}}/p_{\text{amb}}$  is a supportive information for the later pressure and velocity condition in the plasma flow. The ambient pressure is about 1 hPa. It can be seen that very high pressure ratios are achieved leading to the statement that supersonic flows are produced. Checking the well-known one-dimensional equations for nozzles, one gets ratios  $p_{\text{tube}}/p_{\text{amb}} = 15\text{--}20$  taking the applied area ratios of 2, 6, and 4, which confirms the just-mentioned values. The estimative Mach numbers at the nozzle exit are between 2.4 and 2.9.

#### Heat-Flux and Pitot-Pressure Measurements with IPG4-Prototype (50-mm Throat Diameter)

Figure 6 shows measured profiles of heat flux and pitot pressure. The  $\text{CO}_2$  mass flow is 2.7 g/s, and the  $\text{N}_2$  safety flow is 15 g/s. In this campaign no atmospheric  $\text{N}_2$  mass-flow rate was applied. The anode voltage is 6.9 kV, and the anode power is 82 kW. The condition is comparable with case 2 and is therefore called case 2b.

It can be seen that the measured total pressures are up to five times higher than the ambient pressure in the chamber (about 1 hPa). Using an analysis based on the Rayleigh pitot formula, the pressure ratios between 4.5 and 6 lead to Mach numbers between 1.8 ( $x = 115$  mm) and 2.1 ( $x = 55$  mm). This corresponds well with the estimated Mach numbers in the preceding section.

Preliminary tests using aluminum powder with a grain size lower than  $2\text{ }\mu\text{m}$  and  $\text{O}_2$  plasma were performed. This is done as the Martian dust cannot be denied for the planned missions. Even at altitudes of about 40 km, dust particles of 0.1 mm in size can be detected. For aerocapture maneuvers where the entry velocities reach up to 6 km/s, this becomes even more severe.

Anode powers of 100 kW at a  $\text{O}_2$  mass-flow rate of 2 g/s were applied. The aluminum/aluminum oxide layer at the inner tube wall could be seen as the powder has been injected into the gas injection head of IPG3. Meanwhile, tests using iron-oxide dust particles have been performed successfully. The results are presented in Ref. 20.

#### Summary

The design of the inductively heated plasma generator IPG4 and its double-cone nozzle is presented. The results of the experiments prove that a steady-state operation with  $\text{CO}_2$  at very high power is possible. Therefore, the application of IPG4 for  $\text{CO}_2$ -entry simulation is achieved. The calorimetric powers and the local heat fluxes imply very hot  $\text{CO}_2$  plasmas. Together with the modular water-cooled nozzle, the simple and cheap materials used for the plasma generator render IPG4 quite unique in the field of  $\text{CO}_2$  atmospheric entry simulation and TPS testing. The first test using  $\text{O}_2$  with metal powder was promising concerning the intended Mars dust simulation.

Having compared the heat fluxes with figures for typical Mars projects, it can be said that the expected conditions, for example,

for the Mars Sample Return Mission can be achieved. The nozzle satisfies two operational conditions at the same time: High plasma velocities can be achieved while the required mass-flow rate can be drastically reduced. This is not only a matter of cost but also of security as deactivation of the potentially explosive plasma flows becomes less difficult.

#### Acknowledgments

The authors thank all members of the Institute of Space Systems plasma wind-tunnel group. Thanks to S. Laure (Laure Plasma Technology GmbH) for his help and collaboration.

#### References

- Maraffa, L., Smith, A., Santovincenzo, A., Rouméas, R., Huot, J.-P., and Scoon, G., "Aerothermodynamics Aspects of Venus Sample Return Mission," ESA Paper SP 426, Nov. 1998.
- Rubio Garcia, V., Maraffa, L., Scoon, G., Rouméas, R., and Seiler, R., "Mars Mini-Probes. Elements of Aerothermodynamics and Entry Trajectories," ESA Paper SP 426, Nov. 1998.
- Katzkowski, M., and Griebel, H., "Mars Atmosphere Entry of Archimedes Balloon," 3rd International Symposium on Atmospheric Entry Vehicles and Systems, Arcachon, France, March 2003.
- O'Neil, W., and Cazeau, C., "The Mars Sample Return Mission," International Astronautical Federation, Paper 99-Q.3.02, Oct. 1999.
- Auweter-Kurtz, M., Kurtz, H. L., and Laure, S., "Plasma Generators for Re-Entry Simulation," *Journal of Propulsion and Power*, Vol. 12, No. 6, 1996, pp. 1053-1061.
- Auweter-Kurtz, M., Feigl, M., and Winter, M., "Overview of IRS Plasma Wind Tunnel Facilities," Measurement Techniques for High Enthalpy and Plasma Flows Course, RTO EN-8, Rhode-Saint-Génese, Belgium, Oct. 1999, pp. 2A-1-2A-20.
- Herdrich, G., Auweter-Kurtz, M., Kurtz, H., Laux, T., and Winter, M., "Operational Behavior of the Inductively Heated Plasma Source IPG3 for Re-Entry Simulations," *Journal of Thermophysics and Heat Transfer*, Vol. 16, No. 3, 2002, pp. 440-449.
- Herdrich, G., Auweter-Kurtz, M., Kurtz, H., Laux, T., and Schreiber, E., "Investigation of the Inductively Heated Plasmagenerator IPG3 Using Injection Rings of Different Geometries," AIAA Paper 2000-2445, June 2000.
- Laux, T., Herdrich, G., and Auweter-Kurtz, M., "Material and Heat Flux Tests with Sintered Silicon Carbide in Oxygen and Nitrogen Plasmas," *Proceedings of the First Joint French-German Symposium on Simulation of Atmospheric Entries by Means of Ground Test Facilities*, Inst. of Space Systems, Stuttgart, Germany, 1999, Paper 3.3, pp. 3.3-1-3.3-9.
- Bottin, B., Chazot, O., Carbonaro, M., van der Haegen, V., and Paris, S., "The VKI Plasmatron Characteristics and Performance," Measurement Techniques for High Enthalpy and Plasma Flows Course, RTO EN-8, Rhode-Saint-Génese, Belgium, Oct. 1999, pp. 6-1-6-26.
- Gordeev, A. N., "Overview of Characteristics and Experiments in IPM Plasmatrons," Measurement Techniques for High Enthalpy and Plasma Flows Course, RTO EN-8, Rhode-Saint-Génese, Belgium, Oct. 1999, pp. 1A-1-1A-18.
- van Ootegem, B., Leborgne, L., and Vervisch, P., "Experimental Study of a Supersonic Turbulent Low Pressure Argon Plasma Jet," *Proceedings of the 3rd European Symposium on Aerothermodynamics for Space Vehicles*, ESTEC, Noordwijk, The Netherlands, 1998, pp. 105-110.
- Auweter-Kurtz, M., Feigl, M., and Winter, M., "Diagnostic Tools for Plasma Wind Tunnels and Re-Entry Vehicles at the IRS," Measurement Techniques for High Enthalpy and Plasma Flows Course, RTO EN-8, Rhode-Saint-Génese, Belgium, Oct. 1999, pp. 2B-1-2B-78.
- Auweter-Kurtz, M., Herdrich, G., Komurasaki, K., and Laux, T., "Probe Measurements and Laser Absorption Spectroscopy on the IRS IPG3 Plasma Plume," AIAA Paper 2001-2732, June 2001.
- Herdrich, G., Auweter-Kurtz, M., and Kurtz, H. L., "New Inductively Heated Plasma Source for Reentry Simulations," *Journal of Thermophysics and Heat Transfer*, Vol. 14, No. 2, 2000, pp. 244-249.
- Gmelin, L., Becke-Göhrling, M., Buschbeck, K.-C., Kotowsky, A., and Pietsch, E., *Gmelin Handbuch der Anorganischen Chemie*, 8th ed., Gmelin Inst., 1972 (in German).
- Freytag, H. H. (ed.), *Handbuch der Raumexplosionen*, Verlag Chemie GmbH, Weinheim/Bergstr., 1972 (in German).
- Redeker, T., and Schön, G., 6. *Nachtrag zu den Sicherheitstechnischen Kennzahlen Brennbare Gase und Dämpfe*, 2nd ed., Deutscher Eichverlag GmbH, Braunschweig, Germany, 1963 (in German).
- Waters, Ch., "Current Transformers Provide Accurate, Isolated Measurements," Pearson Electronics, Palo Alto, CA, 1999.